Supporting Information

Heim et al. 10.1073/pnas.1614894114

SI Materials and Methods

Mouse Strains and Patient Material. Targeting of embryonic stem cells and mouse chimera production was through the Mayo Clinic Transgenic Core Facility.

Formalin-fixed, paraffin-embedded primary biopsy material was obtained from the Mayo Clinic tissue archive. A discovery cohort of patients (38) was used for a focused examination of the differences in adhesion gene expression between benign cutaneous nevi and melanoma in-transit metastases. This study was approved by the Mayo Foundation Institutional Review Board (11-6390) as a minimal risk study. A patient consent waiver was obtained.

Pharmaceutically Active Compounds and Antibodies. All pharmaceutically active compounds were acquired from Sigma–Aldrich except PF-562271, which was purchased from Selleck (S2890). The following antibodies were used for immunoprecipitation and/or microfluidic Western blot analysis by ProteinSimple (PS), immunohistochemistry (IHC), or immunofluorescence (IF): CD31 (553371, MEC13.3; BD Biosciences; 1:500 for IF), FN (ab2413; Abcam; 1:100 for IHC), Collagen IV (ab6586; Abcam; 1:100 for IHC), Laminin (ab11575; Abcam; 1:100 for IHC, 1:400 for IF), FAK (06-543; EMD Millipore; 1:50 for PS; 1:100 for IF), paxillin (610051, 349; BD Biosciences; 1:100 for IF), phospho-FAK Y397 (AF4528; R&D Systems; 1:200 for PS), phospho-FAK Y397 (44-624G; Thermo Fisher Scientific; 1:100 for IHC), β-tubulin (ab15568; Abcam; 1:50 for PS), SRC (2109, 36D10; Cell Signaling Technology; 1:50 for PS), phospho-SRC Y416 (2101; Cell Signaling Technology; 1:10 for PS), GFP (ab290; Abcam; 1:500 for PS), GST (MA4-004, 8-326; Thermo Fisher Scientific; 1:100 for PS), and Lamin A/C (2032S; Cell Signaling Technology; 1:100 for PS).

NMR Spectroscopy. NMR spectra were recorded at 25 °C on a Bruker AVIII-600 spectrometer with a room temperature probe head. NMR samples were prepared in 25 mM Hepes (pH 7.5) and 200 mM NaCl in 90% H_2O/10% D_2O. A titration experiment was carried out by adding increasing amounts of unlabeled RALPSIPK peptide to a 125 μM MYO1E SH3 sample to a molar excess of 1:7. Assignment experiments were recorded on $^{13}C^{15}N$-labeled samples at a protein concentration of 4 mM. Assignment was carried out by a combination of HNCA, HNCOCA, HNCO, and CCONH spectra, and all backbone resonances could be assigned unambiguously. NMR data were processed using the NMRPipe-NMRDraw software suite, and figures displaying NMR spectra were produced using NMRViewJ (www.onemoonscientific.com). The binding affinity was determined by fitting a single-site model to the CSP data using an in-house written script. CSPs were calculated as given by:

$$\mathrm{CSP} = \sqrt{(CSP_{15N})^2 + (CSP_{1H} * 100)^2}.$$

ITC. Binding constants were determined using a NanoITC instrument (TA Instruments) at 25 °C in buffer containing 25 mM Hepes (pH 7.5) and 200 mM NaCl. RALPSIPK peptide was injected into MYO1E SH3 with stirring at 250 rpm. Measurements were carried out at 1.4 mM MYO1E SH3 and 16 mM peptide and at 0.38 mM MYO1E SH3 and 2.8 mM peptide, respectively. Data were corrected for dilutional heat of the peptide, processed, and integrated using the NanoAnalyze suite (TA Instruments). A single-site model was used for curve fitting in NanoAnalyze.

Plasmids and Constructs. A mammalian expression vector harboring cherry-tagged FAK cDNA (cherry-C1-FAK-HA) was a gift from Anna Huttenlocher, University of Wisconsin School of Medicine and Public Health, Madison, WI (Addgene plasmid 35039). Point mutations were introduced by site-directed mutagenesis using the Quikchange II XL Kit (200521; Agilent Technologies). For stable expression in cell lines, cDNA was cloned into the lentiviral expression vector LV022 (Applied Biological Materials). For recombinant expression of GST-tagged MYO1E, we used plasmid pGEX-5X-3 (GE Healthcare Life Sciences). For recombinant expression of GST-tagged ACTN4, we used plasmid pBP-His-GST (PV567919; Applied Biological Systems).

Primary Cells and Cell Lines. MYO1E-null fibroblasts (lot 3-7) were derived from MYO1E-deficient mice (29) and immortalized using SV40 whole gene (10^6 IU/mL) delivered by lentivirus (G203; Applied Biological Materials) overnight. The $p53^{-/-}$ FAK knockout mouse embryonic fibroblasts (MEFs; CRL-2644) were purchased from the American Type Culture Collection. WM858 melanoma cells ($p53^{-/-}$) were purchased from Meenhard Herlyn (Wistar Institute). M12 melanoma cells ($BRAF^{V600E}$, $NRAS^{WT}$, $KRAS^{WT}$; p53-positive) and M15 melanoma cells ($BRAF^{WT}$, $NRAS^{Q61K}$, $KRAS^{WT}$; p53-positive) were obtained from patient-derived melanoma brain metastases and maintained as patient-derived xenografts. All cell lines were tested for mycoplasma and viral contamination by the RapidMAP 21 test (Taconic) or the Mayo IMPACT Profile (IDEXX BioResearch). Cell lines were cultured in DMEM containing 10% FBS.

To generate WM858 Dual-Glo human melanoma cells (i.e., WM858 cells with a dual-luciferase–tagged endogenous SPP1 promoter), exon 2 (ENSE00003680042) of SPP1 was targeted for a double-strand break using a custom-made zinc finger nuclease (CSTZFN; Sigma–Aldrich). Specifically, the predicted 42-bp zinc finger nuclease-binding site (capital letters) and cutting site (lowercase letters) were as follows: 5′-CTCCTAGGCATCAC-CTGTgccataCCAGTGAGTACAGTTGCA-3′. A donor vector with 500-bp homology arms was cloned so that the SPP1 sequence downstream of the endogenous SPP1 ATG start codon (4: 87,976,896; GRCh38.p7) was replaced with luc2P reporter gene, a luciferase gene that contains hPEST, a protein destabilization sequence cloned from pGL4.15[luc2P/Hygro] (E6701; Promega Corporation). Immediately downstream of luc2P, our donor vector contained a mammalian selectable marker for hygromycin, followed by a CMV promoter-driven hRluc Renilla luciferase gene, intended as a loading control. Correct insertion of the donor cassette downstream of the SPP1 ATG start codon was confirmed by PCR and DNA sequencing. Activity of the SPP1 promoter-driven firefly luciferases and the CMV promoter-driven Renilla luciferase was assayed using the Dual-Glo protocol (E2940; Promega Corporation). The firefly signal was normalized to the Renilla signal and then further normalized to a treatment control. Cells were cultured in the presence of 250 μg/mL Hygromycin B (H0654; Sigma–Aldrich). The luciferase signal was measured using white, flat-bottomed, 96-well plates (CLS3362; Sigma–Aldrich), a Varioskan Flash multimode reader (Thermo Scientific) in luminometric measurement mode, a measurement time of 10 s per well, and SkanIt software version 2.4.3.37.

To generate WM858 melanoma cells with MYO1E shRNA or nontargeting control shRNA, WM858 cells were infected with lentiviral particles containing shRNA derived from the TRC clones TRCN0000151296, TRCN0000152421, and TRCN0000152890 or from nontargeting control in pLKO.1-puro-CMV-tGFP

vector. For targeting *RPS6KB1*, cells were infected with lentiviral particles containing shRNA derived from the TRC clones TRCN0000003162, TRCN0000003161, TRCN0000003160, TRCN0000003159, and TRCN0000003158 or from nontargeting control pLKO.1-puro-CMV-U6 vector. For targeting, *PTK2*/*FAK* cells were infected with lentiviral particles containing shRNA derived from TRC clones TRCN0000194984 and TRCN0000196310 or from nontargeting control pLKO–puro–isopropyl β-D-1-thiogalactopyranoside (IPTG)–1XLacO vector. Of note the *PTK2*/*FAK*-targeting shRNA TRCN0000121207, TRCN0000121318, and TRCN0000121129 were ineffective in WM858 melanoma cells. To induce effective knockdown, cells were cultured in the presence of 50 μM IPTG for at least 5 d. All cells were selected using 0.5 μg/mL puromycin.

Transient and Stable Transfection/Transduction. For transient transfection of WM858 cells, we used Lipofectamine 2000 or 3000 (Thermo Fisher Scientific) according to the manufacturer's protocol. To generate stable cell lines, cells were infected with lentivirus in 2 mL of complete medium containing 8 μg/mL polybrene and a virus multiplicity of infection of 2–20. Selection was by 1–1.5 μg/mL puromycin.

Timed Matings and Embryo Isolation. In all mating procedures, female mice were exposed to male mice overnight. Identification of a vaginal plug the next morning was used to determine E0.5. Staged embryos (E8.5–E16.5) were dissected in ice-cold PBS. Embryos were observed under an Olympus SZX12 Microscope. Small pieces of tail or paw were digested in PBS containing proteinase K at 56 °C for 90 min. Proteinase K was heat-inactivated at 80 °C for 30 min. Two microliters of the sample was used to set up a PCR assay for genotyping.

Whole-Mount 3D Imaging of CD31 in Embryos. Whole-mount 3D imaging of CD31 was performed as previously described (40). To allow for deep penetration of laser light and confocal sectioning, embryos were dehydrated by increasing methanol concentrations, cleared in benzyl alcohol/benzyl benzoate (1:2). Images were obtained with a Zeiss LSM780 confocal microscope using ZEN software (release 8.0).

Coimmunoprecipitation and GST Pull-Downs. For coimmunoprecipitation of FAK, 500 μg of WM858 melanoma cell protein lysate containing GFP-tagged MYO1E in Mammalian Protein Extraction Reagent (MPER; 78501; Thermo Fisher Scientific) was diluted in an equal volume of PBS (28372; Thermo Fisher Scientific) and incubated with Protein G-coated magnetic beads (88847; Thermo Fisher Scientific), which were preincubated with 10 μg of rabbit GFP antibody (ab290; Abcam) or 10 μg of rabbit IgG (12-370; EMD Millipore). Incubation was overnight at 4 °C with gentle rotation. Beads were washed in PBS-diluted MPER (4:1 ratio) gently three times, eluted in PS loading buffer, and run on a Wes microfluidic Western blotting system. For GST pull-down of FAK, 10 μg of recombinant GST-tagged MYO1-SH3 domain [GST-MYO1E(SH3)] or GST-tagged tryptophan (W)-to-lysine (K) mutation at position 1088 (W1088K) mutated SH3 domain [GST-MYO1E($SH3^{WK}$)] was incubated with glutathione magnetic beads (88821; Thermo Fisher Scientific) for 1 h at 4 °C with gentle rotation. Beads were then incubated with cell lysate as described above at 4 °C with gentle rotation overnight, washed in PBS, eluted in PS loading buffer, and run on a Wes microfluidic Western blotting system.

Expression and Purification of Recombinant Proteins. Purified GST-tagged SRC was purchased from Sigma–Aldrich (S1076). GST-tagged Myo1E SH3 domain (wild type or W1088K mutated) in vector pGEX-5X-3 (18) or GST-tagged ACTN4 in vector pBP-His-GST (PV567919; Applied Biological Systems) was expressed in *Escherichia coli* Rosetta 2 cells. Protein-containing bacterial supernatant was applied to a GST Trap FF column (5 mL; GE Healthcare Life Sciences), washed, and eluted. The GST-tagged Myo1E SH3 domain was dialyzed [20 mM Tris, 50 mM NaCl, 2 mM $CaCl_2$ (pH 8.0)] and digested with Factor Xa from New England Biolabs (P8010) at 4 °C for 16 h using 1 μg of the protease to cleave 1 mg of fusion protein. The cleaved protein was isolated by size exclusion chromatography (SEC; SD200/16/60) with SEC buffer [20 mM Hepes, 200 mM NaCl (pH 7.5)] and concentrated to 6 mg/mL. Complex formation was observed on an ETTAN system equipped with a Superdex 200 PC 3.2/30 column using a protein concentration of 1 mg/mL and a 1.6-fold molar excess of the peptide. For circular dichroism measurement, the sample was diluted with deionized water to yield a final concentration of 0.3 mg/mL. Circular dichroism spectroscopy was performed using a JASCO J-720 spectropolarimeter. The mean of 10 protein spectra (300 nm to 190 nm) was corrected by subtracting the buffer spectrum, and the calculated mean residue weight ellipticity was plotted using SciDAVis.

For ^{15}N-labeled protein, a tobacco etch virus (TEV) protease cleavage site was introduced between the GST-tag and Myo1E SH3 domain. This construct was expressed in *E. coli* Rosetta 2 cells using M9 minimal medium supplied with ^{15}N ammonium chloride as the sole nitrogen source and ^{13}C glucose as the carbon source for double-labeled samples. Fusion protein was affinity-purified as described above. After addition of 1 mM DTT and TEV protease, the protein was incubated overnight at 30 °C to cleave the GST-tag. Pure Myo1E SH3 domain was obtained by SEC (SD75/16/60) with SEC buffer.

For pull-downs, synthetic peptides were immobilized on 100 μL of Dynabeads MyOne Streptavidin C1 (65001; Invitrogen) for 1 h at 4 °C and then incubated with 2 μg of recombinant GST-tagged MYO1E protein on a rotator overnight at 4 °C. For competition experiments, 2 μg of MYO1E-GST and 150 μg of synthesized, unconjugated RALPSIPK peptide (FAK amino acids 368–375) or 2 μg of MYO1E-GST and 150 μg of unconjugated scrambled PLAIRKSP peptide were incubated with FAK peptide (amino acids 358–409) coupled to Dynabeads overnight at 4 °C. Beads were washed twice. Protein was eluted by boiling at 95 ° in PS loading buffer for 5 min. Eluates were separated using PS capillaries.

Microfluidic Western Blotting. Western blots were performed as Simple Western assays using the Wes system (PS), a combination of capillary electrophoresis and immunodetection techniques, following the manufacturer's protocols. Quantification of chemiluminescence was based on peak height after correction for a baseline signal. Raw data were generated by Compass software (version 2.5.8–2.7.1, build ID 0201-0826). Compass is the control and data analysis application for Simple Western instruments.

Quantitative Microfluidic PCR. RNA from patient biopsy-derived paraffin sections was extracted and processed as previously described (38). RNA from mouse embryos was isolated using the RNeasy Plus Mini Kit (74134; Qiagen). One microgram of total RNA was transcribed into cDNA using the iScript cDNA Synthesis Kit (170-8891; Bio-Rad). All cDNA derived from paraffin sections or fresh-frozen material was preamplified using TaqMan Preamp Master Mix (4391128; Applied Biosystems). Quantitative reverse transcriptase PCR was then performed using the Fluidigm BioMark HD system and dynamic array-integrated fluid circuits (Fluidigm). Absolute SPP1 and FN RNA copy numbers in mouse embryos or MEFs were determined using copy number standards (38) and normalized to 10^6 copies of housekeeping genes (ACTB and RPL8). For some experiments, absolute copy numbers were normalized to a control group. The following primers were used for mouse-derived cDNA amplification by quantitative PCR: ACTB (1)-forward, GGCTACAGCTTCACCACCAC; ACTB (1)-reverse, TAATGTCACGCACGATTTCC; ACTB (2)-forward, TGACCCAGATCATGTTTGAGA; ACTB (2)-reverse, GTACATGGCTGGGGTGTTG; RPL8-forward, AGGCAAAGAGGAACTGCTG;

RPL8-reverse, GGATGCTCCACAGGATTCAT; SPP1-forward, TGACCCATCTCAGAAGCAGA; SPP1-reverse, TTCTTCAGAGGACACAGCATTC; FN-forward, GTAGGAGAACAGTGGCAGAA; and FN-reverse, GTGCAGGAGCAAATGGC.

Gene Expression by Next-Generation Sequencing. FAK MEF RNA was isolated using the RNeasy Plus Mini Kit. RNA sequencing was performed as previously described (38). Briefly, RNA-derived cDNA libraries were prepared using the TruSeq RNA Library Prep Kit v2 (Illumina). Concentration and size distribution of the resulting libraries were determined on an Agilent Bioanalyzer DNA 1000 chip and confirmed by Qubit fluorometry (Life Technologies). Unique indexes were incorporated at the adaptor ligation phase for three-plex sample loading. Libraries were loaded onto paired-end flow cells to generate cluster densities of 700,000 per square millimeter following Illumina's standard protocol. The flow cells were sequenced as 51 paired-end reads on an Illumina HiSeq 2000 system. The samples were processed through the Mayo RNA-sequencing analysis pipeline, MAP-RSeq. Raw and normalized (reads per kilobase of gene per million mapped reads) gene expression read counts were obtained per sample. Differential gene expression analysis was carried out using the freely available edgeR Bioconductor software package (bioconductor.org). Because scaling by total lane counts can bias estimates of differential expression, edgeR uses trimmed mean normalization on raw read counts to determine whether genes are differentially expressed using the negative binomial method. The Benjamini–Hochberg correction is used to control for multiple testing to obtain a false discovery rate.

Proliferation and Matrigel Invasion Assays. For proliferation analysis, cells were seeded at low densities (2,500–5,000 cells per well). Cells were incubated using an IncuCyte ZOOM (Essen Bioscience). Cell growth based on percent confluence was determined from phase contrast images. For proliferation assays based on automated counting of fluorescent nuclei, cells were first infected with the NucLight Red reagent (4476; Essen Bioscience) and selected using 1 μg/mL puromycin to obtain a stable nuclear red fluorescent label. Invasion assays were performed by seeding cells at a density of 30,000 cells per well on a thin coating of Matrigel (0.1 mg/mL, standard formulation; Corning) in 96-well ImageLock microplates (4379; Essen BioScience). Cells were then allowed to grow confluent. Before scratching, cell proliferation was inhibited by 30 min of exposure to 10 μg/mL mitomycin C (M4287; Sigma–Aldrich). Monolayers were scratched using the WoundMaker pin tool (4493; Essen BioScience). Medium was changed, and cells were covered in 2 mg/mL Matrigel diluted in complete medium. Relative wound density was calculated using the IncuCyte Scratch Wound Cell Migration Software Module (9600-0012; Essen Bioscience).

Immunocytochemistry and IHC. For immunocytochemistry, cells were cultured on LAB-TEK II chamber slides (154453; Thermo Scientific), fixed for 10 min in 4% paraformaldehyde (PFA) at room temperature, and stained with a BOND-MAX autostainer (Leica Biosystems). Briefly, slides were washed with 1× Bond Wash solution (Leica Biosystems), and cells were permeabilized for 10 min with 0.1% Triton X-100 in PBS. After washing and blocking with 3% BSA in PBS for 60 min, slides were incubated with a 1:100 dilution of primary antibody in Bond Primary Antibody Diluent (Leica Biosystems) for 90 min. Slides were washed three times for 2 min each time and incubated with a 1:100 dilution of secondary antibody in Bond Primary Antibody Diluent for 60 min. After three 2-min wash steps, DAPI staining was performed for 10 min. Images were collected at room temperature by confocal microscopy (Zeiss LSM780) with a 40×/1.0-N.A. objective using ZEN software (release 8.0). Colocalization of MYO1E/FAK was highlighted using the ZEN software colocalization algorithm using arbitrary cutoffs. For IHC on paraffin sections using phospho-FAK Y397 antibody (44-624G), sections were baked, dewaxed, and exposed to EDTA-based pH 9.0 solution (AR9640; Leica Biosystems) using a BOND-MAX autostainer. Antibody detection was by alkaline phosphatase-linked polymers (DS9390; Leica Biosystems). For IHC on frozen sections using laminin, collagen, or FN antibodies, epitope retrieval was not required. Antibody detection was by secondary Alexa 488-conjugated antibody (1:200 dilution). Stained paraffin sections were digitalized with an Aperio ScanScope (Leica Biosystems). For FAK phospho-Y397–stained slides, an overview and a maximum magnification image were imported into Microsoft Powerpoint (version 14) per case. To generate contrasted images of FAK phospho-Y397 versus background, maximum magnification images were converted to 75% black and white, brightness was set to 50%, and contrast was set to 100%.

Postembedding Immunogold Electron Microscopy. Cells were fixed in 4% PFA + 2% sucrose. Following fixation, channels were rinsed with 0.1 M phosphate buffer (pH 7.0), dehydrated through a graded series of ethanol, and embedded in LR Gold Resin (EMS). Ultrathin sections (0.09 μm) were labeled with FAK (06-543; EMD Millipore) or GFP antibodies (ab290; Abcam) and with 10 nm of gold-conjugated IgG secondary antibodies (EMS). Micrographs were acquired using a JEOL1400 Plus transmission electron microscope operating at 80 kV.

ChIP-Seq. DNA–protein complexes in WM858 melanoma cells were cross-linked using fresh 1% formaldehyde for 10 min at room temperature, followed by glycine quenching (125 mM for 5 min at room temperature). Approximately 10^6 cells were harvested and lysed by incubating in 10 mM Tris·HCl (pH 7.5), 10 mM NaCl, and 0.5% Nonidet P-40 lysis buffer for 10 min at 4 °C. Chromatin was first fragmented using micrococcal nuclease at 2000 gel units/mL (New England Biolabs) in 20 mM Tris·HCl (pH 7.5), 15 mM NaCl, 60 mM KCl, and 1 mM $CaCl_2$ digestion buffer at 37 °C. After 20 min, the reaction was stopped with 100 mM Tris·HCl (pH 8.1), 20 mM EDTA, 200 mM NaCl, 2% Triton X-100, and 0.2% sodium deoxycholate buffer. The chromatin was further fragmented using a Bioruptor sonicator (Diagenode) set at the "high" setting. Fragment sizes were determined using an Advanced Analytical Technologies Fragment Analyzer Automated CE System. Chromatin preparations were reacted with antibodies against FAK (06-543, EMD Millipore; C20, Santa Cruz Biotechnology) or mCherry (ab183628; Abcam) overnight at 4 °C and precipitated using Protein G agarose beads (Roche Diagnostics). After elution of DNA–protein complexes, cross-links were reversed by proteinase K digestion overnight at 62 °C and DNA was purified using the Qiagen PCR Purification Kit. Sequencing libraries were constructed using the NuGEN Ovation Ultralow DR Multiplex System 1-8 (NuGEN Technologies). Briefly, the DNA fragments underwent end repair, barcoded sequencing adapter ligation, purification (Agencourt RNAClean XP beads; Beckman Coulter), and PCR amplification (13 cycles). Final ChIP libraries were sequenced (paired-end, 51 bases per read) on the Illumina HiSeq 2000 platform. Data were analyzed using the HiChIP pipeline. Briefly, paired-end reads were mapped by the Burrows-Wheeler Aligner (BWA) software package, and pairs with one or both ends uniquely mapped were retained. Peaks were called for these samples using the MACS2 software package at a false discovery rate of ≤1%. For data visualization, Bedtools was used in combination with in-house scripts to generate a normalized tag density profile at a window size of 200 bp and step size of 20 bp. Data were visualized using Integrative Genomics Viewer (IGV). The peaks called by MACS2 for all of the samples were multi-intersected using Bedtools to obtain a list of shared peaks that were detected in more than one ChIP experiment. The list of peaks was filtered to remove peaks in the blacklist regions, which may be false peaks because of satellites, telomere repeats, and centromere repeats [blacklist regions from the Encyclopedia of DNA Elements (ENCODE)]. Retained peaks were assigned to genes if they were present

in ±2 kb around the translation start site. The MEME Suite was used to discover novel DNA-binding motifs from the peak regions, which were called outside the blacklist regions. The peak region for this analysis was obtained from ±100-bp regions around each peak center. The width of the motif was constrained between 7 and 10 bp.

FAK Kinase Assay. To assay kinase activity, we used the ADP-Glo Kinase Assay method (V9101; Promega) in combination with the FAK Kinase Enzyme System (V1971; Promega), which included recombinant FAK kinase domain amino acids 393–698 using the manufacturer's instructions. Full-length recombinant FAK from baculovirus-infected Sf9 cells was obtained from Abcam (ab105909). A 10% ATP-to-ADP conversion at a 100 μM concentration using full-length FAK (SB10 value) at room temperature and 90 min of incubation was achieved by 65 ng of enzyme. To calculate the percentage of enzyme activity, we first subtracted the signal of the negative control (no enzyme and no MYO1E SH3) from sample signals. The 100% kinase activity signal (no MYO1E SH3) was used to calculate fold change in the presence of MYO1E SH3 titration.

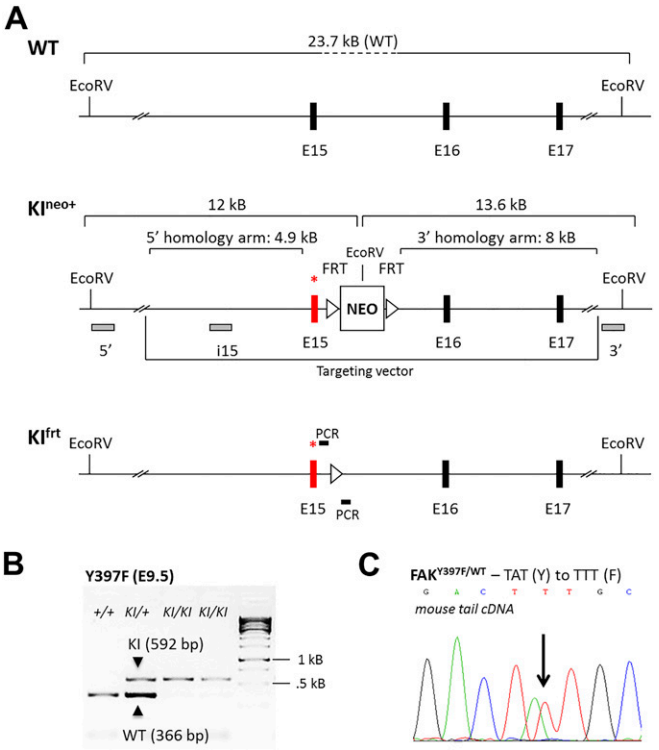

Fig. S1. Generation of FAKY397F knock-in (KI) mice. (*A*) Partial map of the FAK allele. Exon 15 (E15), which contains mutated Y397, is marked by an asterisk, before (KI^{neo+}) and after (KI^{frt}) flippase-mediated deletion of the flirted (FRT) neocassette. The DNA fragment sizes obtained after EcoRV restriction digest, as well as probes (5′ and 3′ probes external to the targeting vector and the i15 internal probe) used for Southern blotting are shown. Filled boxes indicate exons, and triangles indicate FRT sites. Location of PCR primers for KI^{frt} mice genotyping is depicted: forward, GCTTTAGAGCACATCTGTCAC; reverse, CTGGGCTGCTTGAATAGTGGG. NEO, neomycin resistance gene; WT, wild-type. (*B*) Representative PCR genotyping of KI^{frt} embryos at E9.5 using primers flanking the FRT site. The expected PCR product size is 592 bp for the KI allele and 366 bp for the WT allele. PCR results from WT embryos ($^{+/+}$), heterozygous embryos (KI/$^{+}$) and homozygous embryos (KI/KI) are shown for both of the Y397F KIs. kB, kilobase. (*C*) Sanger sequencing of cDNA derived from the tails of heterozygous KI mice. Double peaks are indicative of base pair changes in the respective KI alleles. Y, tyrosine codon sequence; F, phenylalanine codon sequence.

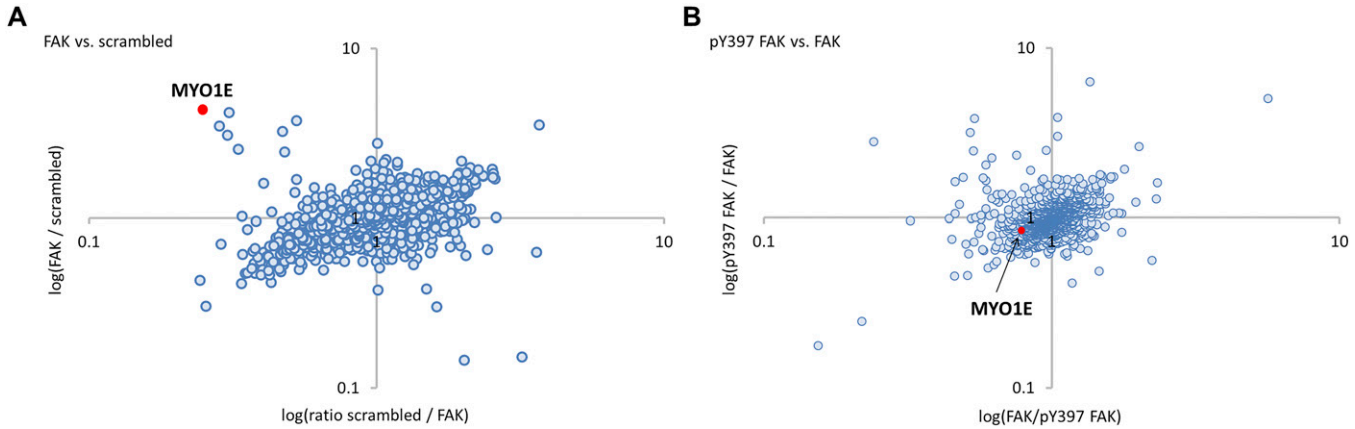

Fig. S2. MYO1E binds equally well to Y397-phosphorylated FAK peptide and nonphosphorylated FAK peptide. (*A*) Scatter plot of nonphosphorylated FAK FERM-kinase domain linker peptide versus scrambled peptide pull-down results using WM858 melanoma cell lysate. The log SILAC ratio of proteins identified with at least two unique peptides in each mass spectrometry run is plotted as the forward pull-down (*x* axis) against the reverse labeling pull-down (*y* axis). MYO1E binds with a high ratio to nonphosphorylated WT FAK peptide over scrambled peptide. (*B*) Scatter plot of Y397-phosphorylated FAK FERM-kinase domain linker peptide versus nonphosphorylated FAK peptide pull-down results using WM858 melanoma cell lysate. Forward and reverse pull-downs result in MYO1E SILAC ratios around 1, indicating equal binding of MYO1E to both peptides.

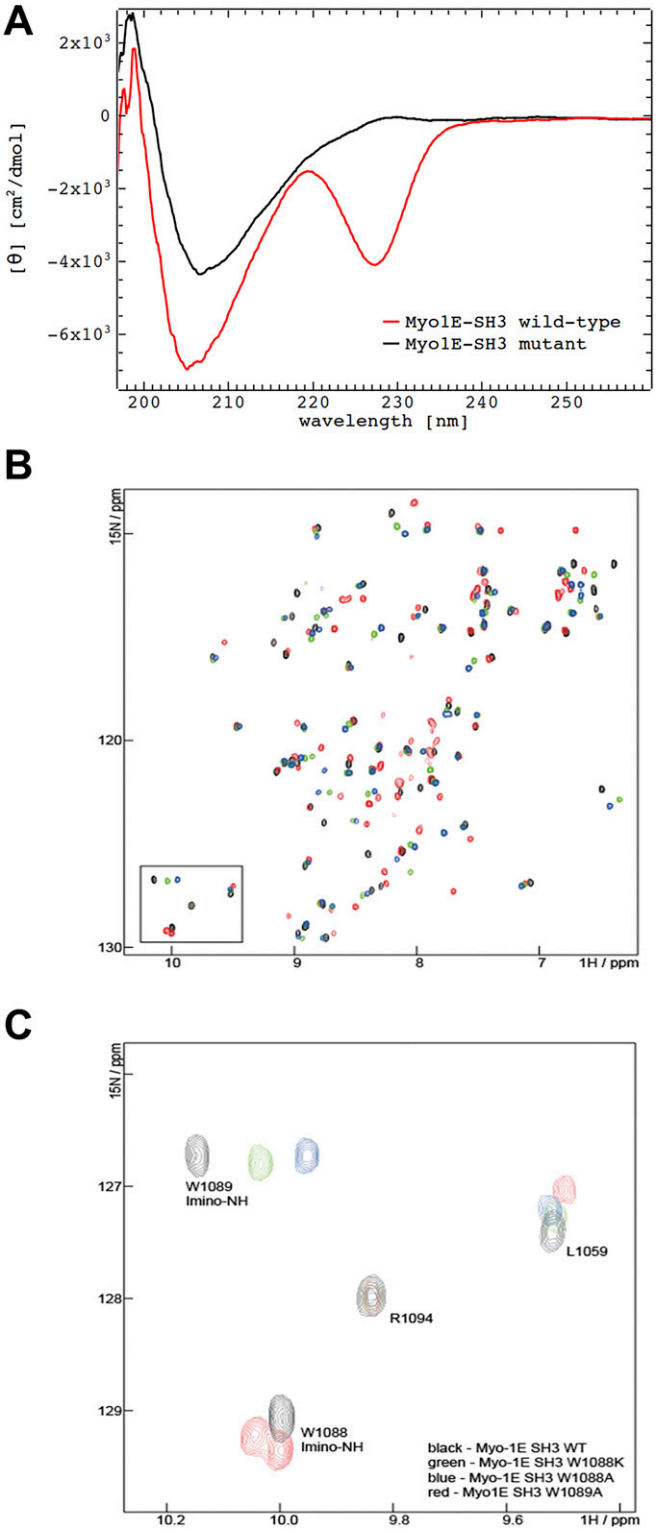

Fig. S3. Assessment of folding of recombinant MYO1E SH3 domains by circular dichroism and NMR. (*A*) Circular dichroism spectra of recombinant WT and W1088K MYO1E SH3 domains (after GST-tag removal). Results indicate folded proteins. (*B* and *C*) Assignment of the tryptophane side-chain imine peaks: NMR spectra of MYO1E SH3 WT (black), W1088A (blue), 1088K (green), and 1089A (red) in the absence of peptide. (*B*) Overlay of the spectra in the imino region demonstrates that the bottom imino peak is absent in the spectra of W1088A and W1088K, thus indicating that this peak corresponds to W1088. Vice versa, the top imino peak is absent in W1089A. In this mutant, the W1088A peak displays peak splitting, which can be attributed to the poorer spectral quality of this mutant. (*C*) Overlay of the whole spectra of Myo-1E SH3 WT and tryptophane mutants. The spectra of W1088A and W1088K display well-dispersed peaks that partially overlap with the WT protein. This finding indicates that these mutants are well folded and adopt the same fold as the WT protein. The spectrum of W1089A (red) displays poorer spectral quality and some peak splitting.

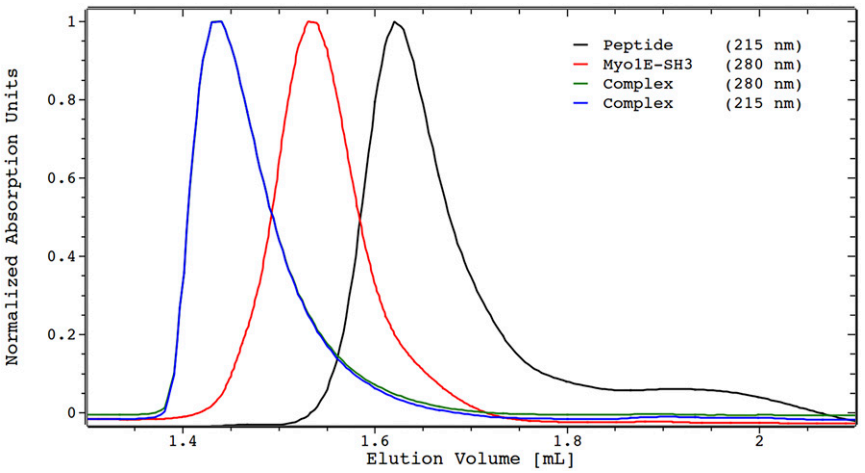

Fig. S4. Analytical SEC demonstrates complex formation between the recombinant MYO1E-SH3 domain (after GST-tag removal) and RALPSIK peptide in solution.

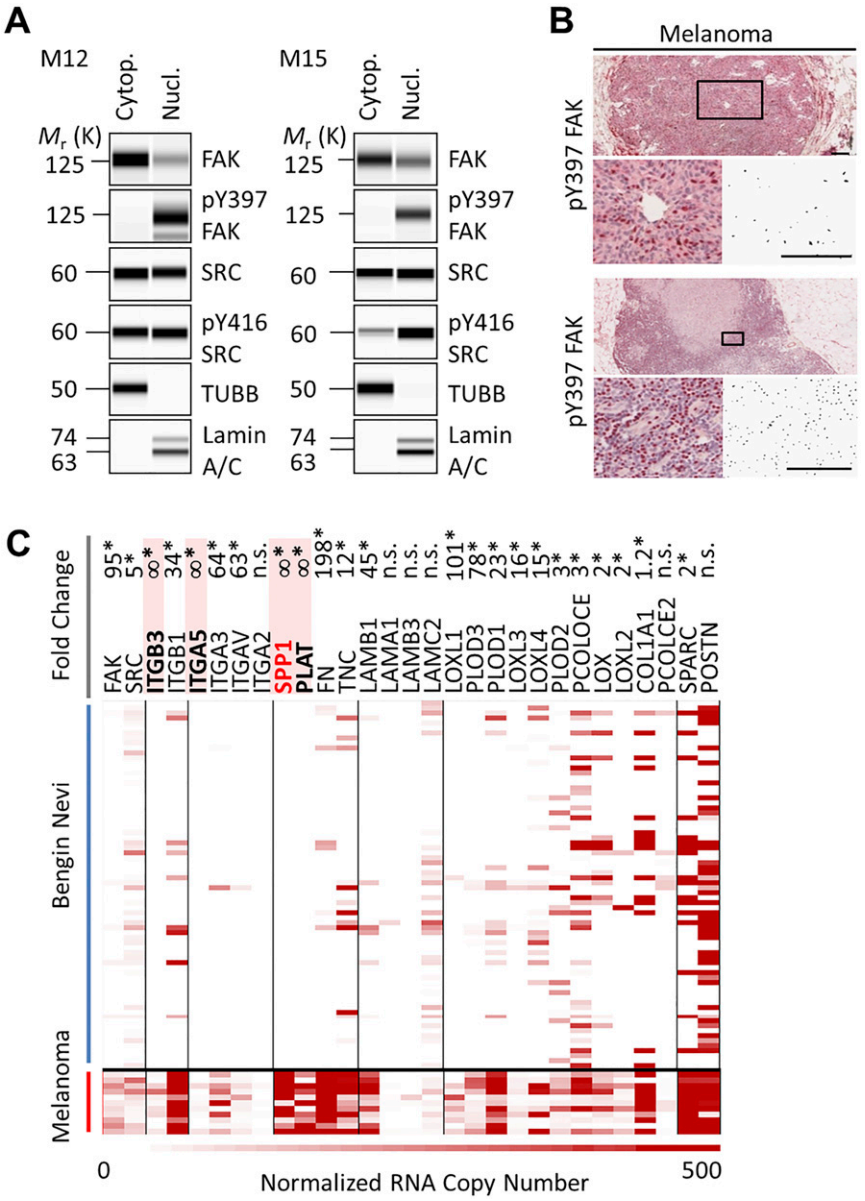

Fig. S5. (*A–C*) Nuclear localization of phospho-Y397 FAK correlates with FN-type gene expression in melanoma. Cytop. cytoplasm; Nucl., nuclear.

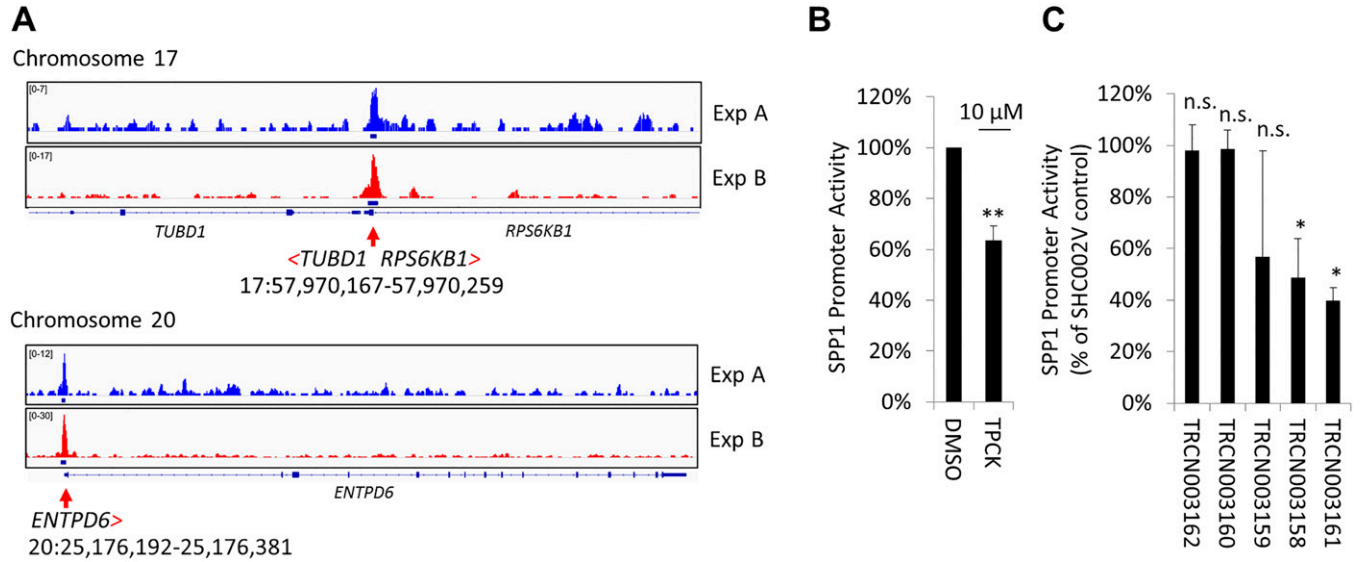

Fig. S6. FAK ChIP-seq in WM858 melanoma cells. We sought to determine whether FAK associates with specific promoters in WM858 cells by using ChIP-seq. Three FAK antibodies detected 182 partially overlapping peaks in six ChIP-seq experiments, and 74 were detected in two independent experiments. (*A*) Exemplary promoter regions identified with high fidelity and within 2 kb of the transcription start site are shown and include the *RPS6KB1* promoter. Based on 182 peaks detected, we determined the following consensus binding sequence: GCGC[AC]TGCGC. This binding sequence is highly similar to the optimal binding site for nuclear respiratory factor 1 (NRF1), (T/C)GCGCA(C/T)GCGC(A/G), which activates the expression of key metabolic genes. (*B*) To test whether the *RPS6KB1* gene product, ribosomal S6 Kinase 1 (S6K1), helps drive SPP1 promoter activity, we exposed WM858 Dual-Glo cells to *N*-p-Tosyl-L-phenylalanine chloromethyl ketone (TPCK), a p70S6 kinase inhibitor. TPCK inhibited SPP1 promoter activity by ∼40%. SPP1 promoter activity after overnight TPCK treatment of WM858 cells is shown (mean ± SD; $n = 3$; $^{**}P < 0.001$). (*C*) Likewise, two of five *RPS6KB1*-directed TRC shRNAs significantly inhibited SPP1 promoter activity. Effects of various TRC clone-derived *RPS6KB1* shRNAs on SPP1 promoter activity are shown (mean ± SD; $n = 2$; $^{*}P < 0.05$). n.s., not significant.

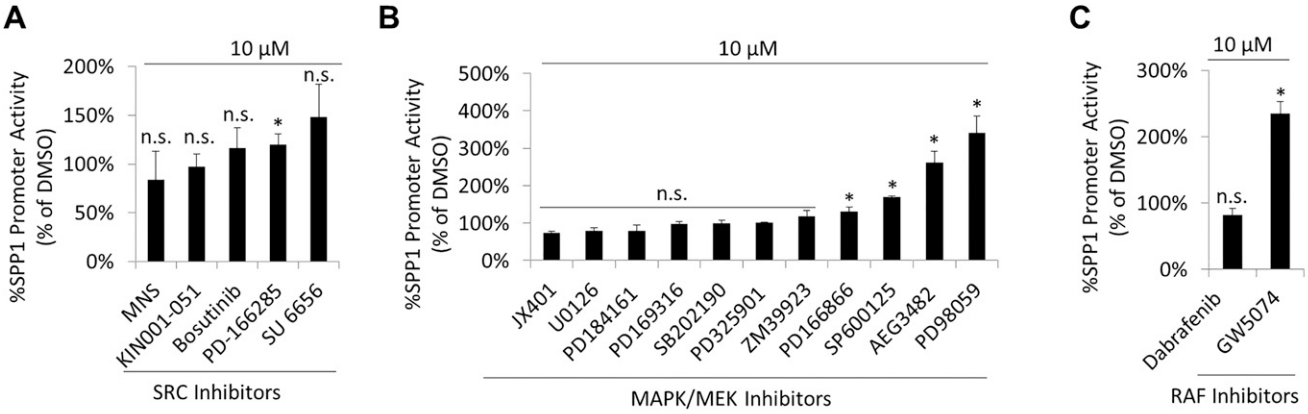

Compound	Description
SRC	
MNS	3,4-Methylenedioxy-beta-nitrostyrene; Src and Syk kinase inhibitor; prevents phosphorylation and cytoskeletal association of GPIIb/IIIa and talin
KIN001-051	7-Cyclopentyl-5-(4-phenoxy)phenyl-7H-pyrrolo[2,3-d]pyrimidin-4-ylamine; potent and selective Ick (src family tyrosine kinase) inhibitor
Bosutinib	Bosutinib (SKI-606) is an orally active; dual Src/Abl tyrosine kinase inhibitor with potent antiproliferative activity
PD-166285	PD-166285 hydrate is a broad spectrum protein tyrosine kinase inhibitor; Src and FGFR kinase inhibitor
SU 6656	Selective Src family kinase inhibitor
MAPK/MEK	
JX401	Potent, non-cytotoxic, membrane permeable p38a MAPK inhibitor
U0126	Specific inhibitor of MEK1 and MEK2 (MAP kinase kinase; MAPKK); also inhibits a constitutively active, mutant form of MEK
PD184161	MEK inhibitor
PD169316	Potent, cell permeable and selective p38 MAP kinase inhibitor; nM potency
SB202190	Highly selective, potent and cell permeable p38 MAP kinase inhibitor
PD325901	PD0325901 is a potent MKK1 (MEK1) and MKK2 (MEK2) inhibitor
ZM39923	JNK-3 inhibitor
PD166866	PD-166866 is a selective inhibitor of the FGF-1 receptor tyrosine kinase (FGFR1) with IC50 = 55 nM, and no effect on c-Src, PDGFR-b, EGFR or insulin receptor tyrosine kinases or MEK, PKC, and CDK4
SP600125	Selective c-Jun N-terminal kinase (c-JNK) inhibitor
AEG3482	AEG3284 is a compound that binds to HSP90, leading to heat shock factor 1 (HSF1) dependent expression of HSP70, an endogenous inhibitor of JNK activity
PD98059	Specific inhibitor of the activation of mitogen-activated protein kinase kinase (MAPKK)
RAF	
Dabrafenib	selective Raf kinase inhibitor that inhibits the kinase activity of wild-type B-Raf, B-Raf V600E and c-Raf
GW5074	cRaf1 kinase inhibitor

Fig. S7. MAPK pathway does not drive SPP1 expression in WM858 melanoma cells. SPP1 promoter activity after exposure of WM858 Dual-Glo cells to SRC inhibitors (*A*), MAPK/MEK inhibitors (*B*), or RAF inhibitors (*C*) overnight is shown (mean ± SD; $n = 3$; $*P < 0.05$). A brief description of compounds used is provided. *P* values, Student's *t* test.

Table S1. Genotypes of embryos obtained from crosses between FAK Y397F/$^{+}$ heterozygous mice derived from ES cell clone 64

Genotype*	E9.5	E10.5	E11.5	Born (P0)
$^{+/+}$	38	33	12	229
$^{+}$/KI	54	52	29	471
KI/KI	29	24	2	0
No. of litters	15	13	6	100

The total number of embryos of each genotype obtained from crosses between mice (FAK Y397F/+; ES cell clone 64) is shown at various embryonic days (E) and at birth (P0).
*KI = FAK^{Y397F}.

Table S2. Genotypes of embryos obtained from crosses between FAK Y397F/$^{+}$ heterozygous mice derived from ES cell clone 354

Genotype*	Born (P0)
$^{+/+}$	21
$^{+}$/KI	37
KI/KI	0
No. of litters	8

The total number of mice of each genotype (FAKY397F/+; ES cell clone 354) at birth (P0) is shown.
*KI = FAK^{Y397F}.

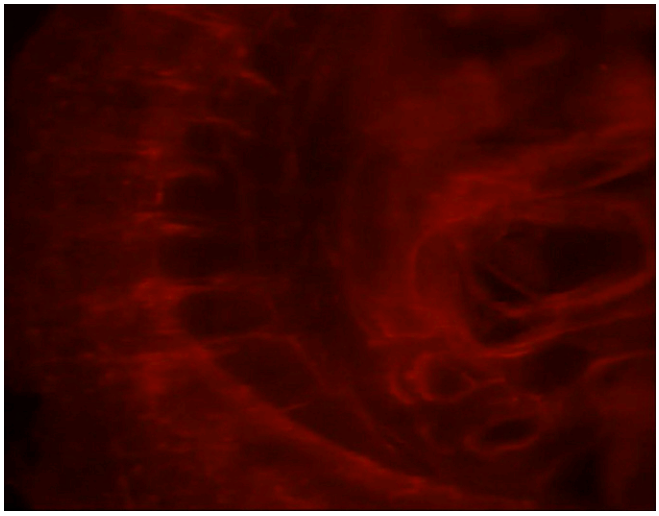

Movie S1. Whole-mount 3D imaging of CD31-immunostained blood vessels in a wild-type embryo at E10.5. Rotation is around the cranial (image top)-to-caudal axis. The dorsal aorta (DA) is visualized as well as intersomitic vessels originating from the DA branching toward the somites. A web of smaller vessels can be identified in and around the somites.

Movie S1

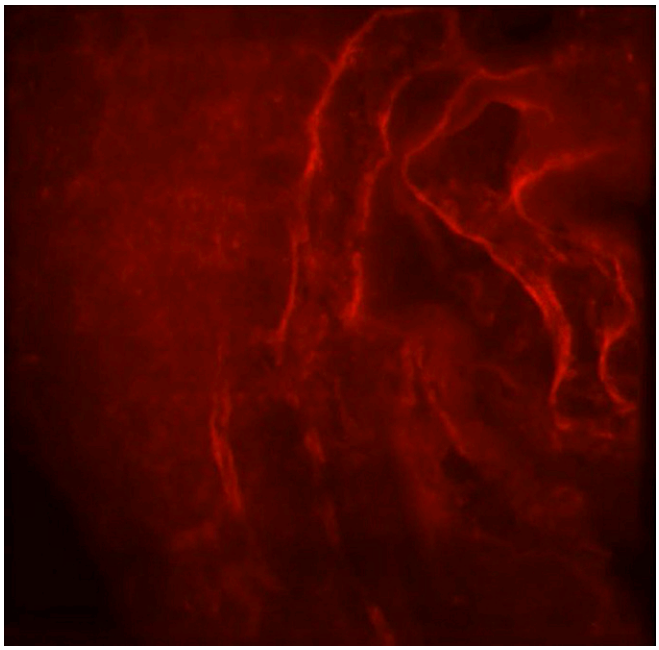

Movie S2. Whole-mount 3D imaging of CD31-immunostained blood vessels in a FAK Y397F embryo at E10.5. Rotation is around the craniocaudal axis (top down on movie). The DA is visualized as well as heart structures. Intersomitic vessels are not seen, however. Also, there is no web of smaller vessels in the area of somites as is observed in wild-type embryos.

Movie S2

Dataset S1. List of genes induced by FAK as determined by total RNA sequencing

Dataset S1